HTS Josephson junctions arrays for high-frequency mixing

A Sharafiev[1] , **M Malnou**[1]**, C Feuillet-Palma**[1] **, C Ulysse**[2]**, T Wolf**[1]**, F Couëdo**[1]**, P Febvre**[3]**, J Lesueur**[1] **and N Bergeal**[1]

[1] Laboratoire de Physique et d'Etude des Matériaux, CNRS, ESPCI Paris, PSL Research University, UPMC, Paris, France
[2] Centre de Nanosciences et de Nanotechnologie, CNRS, Université Paris Saclay, Marcoussis, France
[3] IMEP-LAHC, CNRS, Université Savoie Mont Blanc, Le Bourget du Lac, France

E-mail: jerome.lesueur@espci.fr

CrossMark

Abstract
We designed, fabricated and measured short one-dimensional arrays of masked ion-irradiated $YBa_2Cu_3O_7$ Josephson junctions embedded into log-periodic spiral antennas. They consist of four or eight junctions separated either by 960 nm or 80 nm long areas of pristine material. Large spacing arrays show 'giant' Shapiro steps in the hundreds-GHz band at 66 K and are tested as Josephson mixers with improved impedance matching. On the contrary, small spacing arrays behave as one junction with a lower superconducting transition temperature, hence forming a single weak link on distances up to 880 nm. Such design opens a new way to increase the I_cR_n product of the devices, and therefore the efficiency of Josephson mixers. Hints on the origin of the observed long range proximity effect are proposed.

Keywords: Josephson junction, Josephson junctions arrays, high-T_c superconductor, Josephson mixing, proximity effect

(Some figures may appear in colour only in the online journal)

1. Introduction

While high temperature superconductors (HTSCs) have been identified as promising materials to make high-frequency (THz) Josephson devices for a long time, recent spectacular developments in the field are making this happen for real [1–3]. The era of THz devices based on HTSc Josephson junctions (JJs) is opening, and one can explore the potentialities of different techniques able to produce them.

The ion irradiation technique is a promising approach for manufacturing HTSc integrated circuits [4, 5]. It allows the design of a large number of planar JJs arbitrarily located on a single superconducting film, and therefore offers a natural scalability compared to other types of HTSc junctions. This technique was first introduced by Tinchev [6] to make RF-SQUIDs. Since then, many other applications have been suggested: DC SQUIDs [7], superconducting interference filters (SQIFs) [8, 9], and Josephson mixers [10, 11]. Further developments of this technology have been explored, with other materials such as MgB_2 [12], and more recently by

using a He focused ion beam to directly create disorder at a nanoscale to make a JJ [13, 14].

The main drawback of the technology for high-frequency mixing is the fairly low impedance of the JJ. The normal resistance R_n of an ion-irradiated junction is typically of the order of a few ohms for standard geometries ($\sim \mu$m), which does not match the characteristic impedance Z_0 (=50 Ω of the readout microwave setup. In Josephson mixers, this has been identified as the main reason for moderate conversion efficiency [10, 11]. This is also an issue for SQUID and SQIF applications, to obtain a large voltage signal.

One possible way to overcome the problem consists in replacing a single JJ by an array of JJs in combination with planar coupling structures. Such Josephson junction arrays (JJAs) have in addition several advantages that have been described theoretically in the 1980s ([15] and references therein), such as a reduced line-width [16] and an enhanced emitted power for instance. Operating prototypes of HTSc array-based devices for different applications have been developed: voltage standard [17, 18], wave form generators

[19], detectors and mixers [20, 21], for which long range synchronisation of the JJ has been studied [18, 22–25].

Ion-irradiation technology is capable of delivering reliable arrays on a large scale [8, 9, 26–28], with up to 36 000 JJs in SQUID and SQIF devices [28], and suitable for obtaining giant Shapiro steps [26, 29] when put in series. A unique property of irradiation technology lies in the possibility of fabricating very densely packed JJAs while keeping a planar geometry. Unlike other types of HTSc arrays, the distance between two adjacent JJs can be on the order of the relevant physical scales such as the proximity effect coherence length ξ_N, typically a hundred nanometers [26, 29, 30]. It is therefore possible to explore different coupling regimes between closely packed JJs, and to address the question of the synchronisation mechanism in these situations [31].

In this article, we report on the experimental results of small ion-irradiated JJAs, where the distance between single JJs has been varied from 80 to 960 nm. We clearly identify two regimes: in closely spaced JJ devices, the whole array behaves as a single JJ through a giant proximity effect, while in distant JJ ones, large Shapiro steps are observed as expected for independent JJs in series. Mixing the properties of these devices has been studied, together with the physics of closely spaced JJs.

2. Experiments

The test-bed geometry that we use to explore the properties of the ion-irradiated JJA is a Josephson mixer. As in our previous studies [10, 11], the active element (JJ or here a JJA) is embedded in a spiral log-periodic antenna which is inserted in a 50 Ω coplanar waveguide (CPW) transmission line (figure 1(a)). Heterodyne detection is performed by sending the signal and a local oscillator (LO) reference signal onto the antenna (typically in the tens or hundreds GHz range), and by detecting the intermodulation signal at the intermediate frequency (IF), in the GHz range through the CPW line. Impedance matching with the 50 Ω line and the antenna is a key condition to optimise the conversion efficiency from the high-frequency signal to the IF one.

Details of our standard fabrication technique can be found in Bergeal *et al* [32] and Malnou *et al* [11]. The main steps are illustrated in figures 1(a)–(f), and an optical picture of a N = 8 JJA with a spacing S = 80 nm is presented in figure 1(g). In short, we start from a commercial 70 nm thick $YBa_2Cu_3O_7$ film grown on a sapphire substrate[4], and covered with a 250 nm gold layer. The spiral antenna and the CPW transmission line are first defined in the gold layer through a ma-N e-beam patterned resist[5], followed by a 500-eV Ar^+ ion beam etching. Then a 2 μm wide channel located at the centre of the antenna is patterned in a ma-N e-beam resist, followed by a 70 keV oxygen ion irradiation at a dose of $1 \cdot 10^{15}$ at/cm^2. This process ensures that the regions of the film which are not protected either by the resist or by the gold layer become

insulating. Finally, the junction array is defined by irradiating the superconducting channel through 40-nm wide slits patterned in a PMMA (Poly(methyl methacrylate)) resist, with 110 keV oxygen ions at a dose of $3 \cdot 10^{13}$ at./cm^2.

Stopping and range of ions in matter (SRIM) simulations[6] have been used to evaluate the defect density generated by the ion irradiation. A typical example is displayed in figure 1(h), where the irradiation is performed through two 40 nm wide slits located 80 nm apart. Defect density expressed in dpa (displacement per atom, colour scale) is shown within the sample. While it reaches dpa$\sim$0.01 in the centre of the slits, and therefore locally decreases T_c to form the JJ, it is almost null in the intermediate region. We designed JJA in this limited case, with four and eight JJs in series, and JJA with 960 nm spacing, with the same number of JJs. Thirteen samples have been measured, and the results that we present here are typical of the whole series.

The samples were placed inside a closed cycle refrigerator, at the focal point of a Winston cone, and then exposed to the external signals through an optical window. CPW lines were connected to microwave readout lines through a printed-circuit board. The signals in the 4–8 GHz bandwidth were first amplified at cryogenic temperature by a high-electron-mobility transistor low noise amplifier, before further amplification at room temperature. An isolator was placed between the sample and the first amplifier to minimise the back action noise [11]. DC output voltage and AC output power at intermediate frequency P$_{IF}$ were measured as a function of the applied bias current and temperature.

3. Arrays with Josephson junctions 960 nm apart

First, we focus on the situation where the distance between the slits is much larger (S = 960 nm) than the typical 80 nm straggling of the ions calculated by SRIM (see figure 1(h)), so that the damaged areas do not overlap. In that case junctions can thus be considered as independent . In figure 2 we show the resistance R and the Josephson critical current I_c as a function of temperature for arrays with four and eight JJs. As expected, R(8 JJ) $\sim$ 2 $\times$ R(4 JJ) and the critical currents look very similar. The coupling temperature T$_J$ $\sim$ 70 K below which Josephson coupling takes place is the same for both samples, and corresponds to the one of a single JJ irradiated in the same conditions. For a given spacing (here S = 960 nm), the spread in T$_J$ among the samples is 1 to 2 K maximum. The spread in resistance and critical current among the samples for a given geometry is $\sim$10%. This points towards rather homogeneous JJ characteristics within the arrays. The I–V characteristics are resistively shunted junction (RSJ) like (see inset figure 2) as known for single ion-irradiated JJ [5, 9, 11, 32].

The homogeneity is confirmed by the observation of 'giant Shapiro steps' under microwave irradiation. Figure 3(a) shows the I–V characteristics of a 4 JJ array under irradiation at $f = 20$ GHz. Shapiro steps correspond to 4 JJ in series
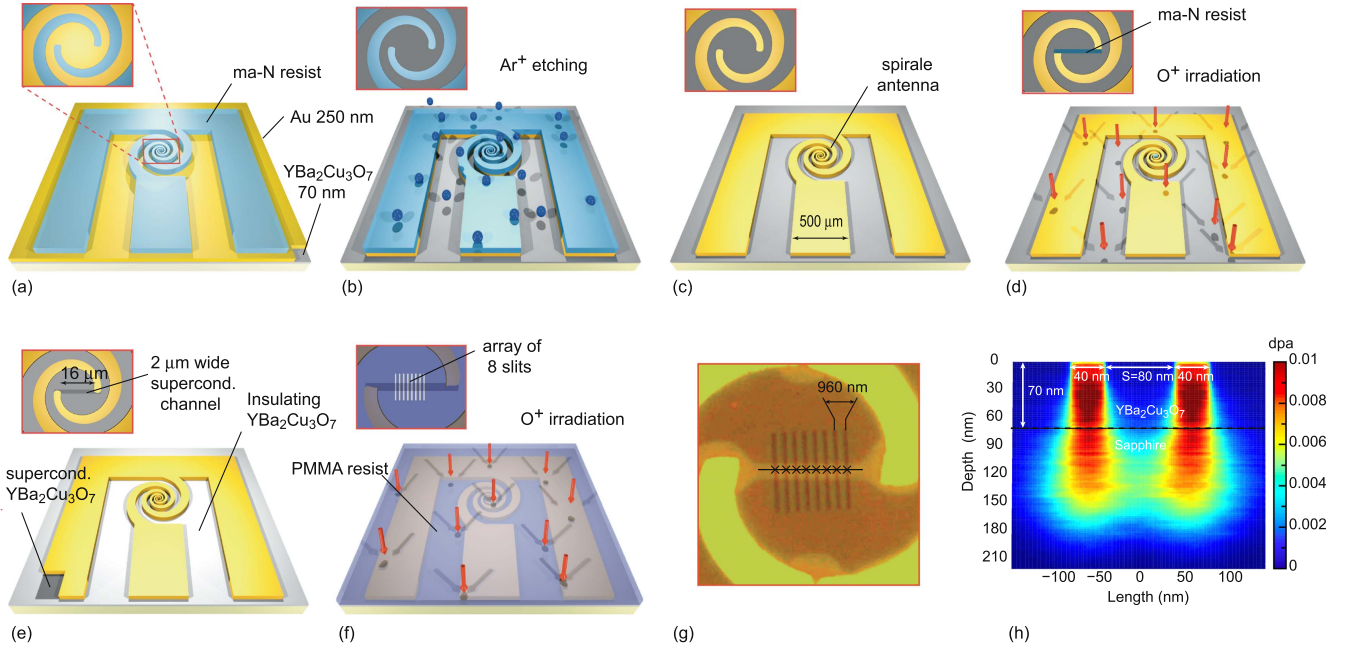
Figure 1. Illustration of the fabrication process steps: (a) spiral antenna and CPW transmission line patterned in a 500 nm thick ma-N negative e-beam resist. The sample consists of a 70-nm thick $YBa_2Cu_3O_7$ film grown on sapphire covered by an *in situ* 250-nm gold layer; (b) 500-eV Ar ion-beam-etching of the gold layer; (c) gold antenna in the CPW transmission line on $YBa_2Cu_3O_7$; (d) high-dose 70-keV oxygen ion irradiation to create insulating regions in exposed $YBa_2Cu_3O_7$. A 2-μm wide channel in the centre of the antenna is protected by a 500 nm thick ma-N resist mask; (e) patterned superconducting and insulating $YBa_2Cu_3O_7$ regions; (f) low-dose 110 keV oxygen ion irradiation of the eight Josephson junctions array patterned as 40-nm-wide slits in a 500 nm thick PMMA resist; (g) optical picture of an array of eight 40 nm wide slits separated by 960 nm, opened in the PMMA resist. The apparent size of the slits is limited by diffraction. Black crosses shows the 8 JJ in series; (h) SRIM simulation of the defect density (dpa, colour scale) in a 70 nm thick $YBa_2Cu_3O_7$ film deposited on sapphire substrate, irradiated with $3 \cdot 10^{13}$ at./cm^2 through 40 nm wide slits separated by a spacing S = 80 nm.
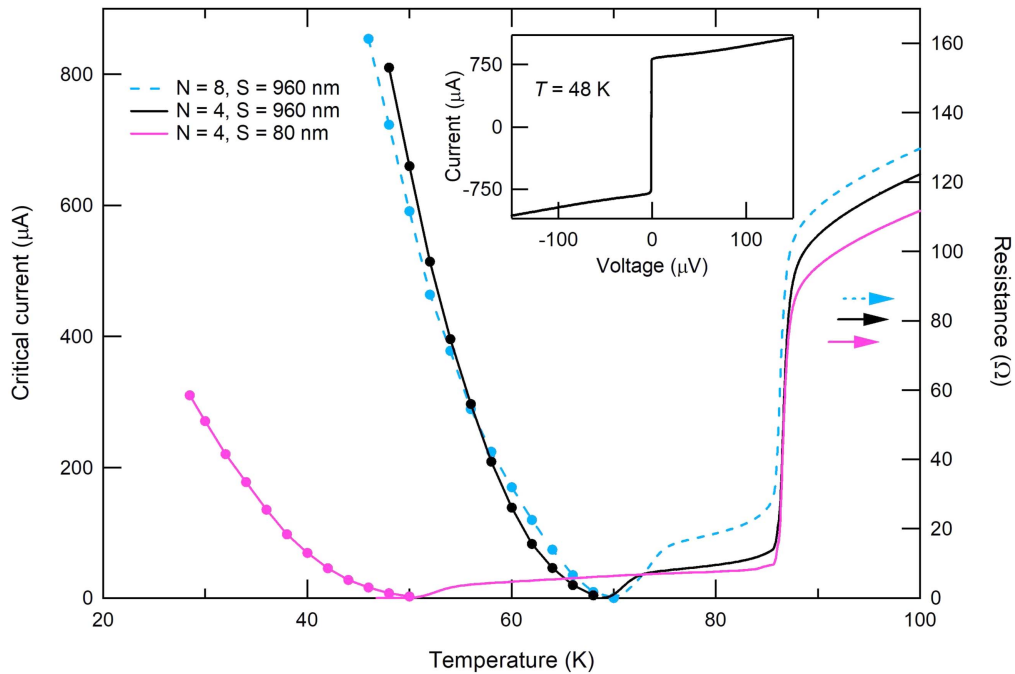

Figure 2. Temperature dependence of the resistance (lines, right scale) and the critical current (symbols, left scale) of JJAs with N JJ in series, separated by a spacing S. The transition temperatures T_J are $\sim$70 K and $\sim$50 K or S = 960 and 80 nm, respectively. Inset: I-V characteristics of a 4 JJ array with S = 960 nm spacing measured at 48 K, which is RSJ like.
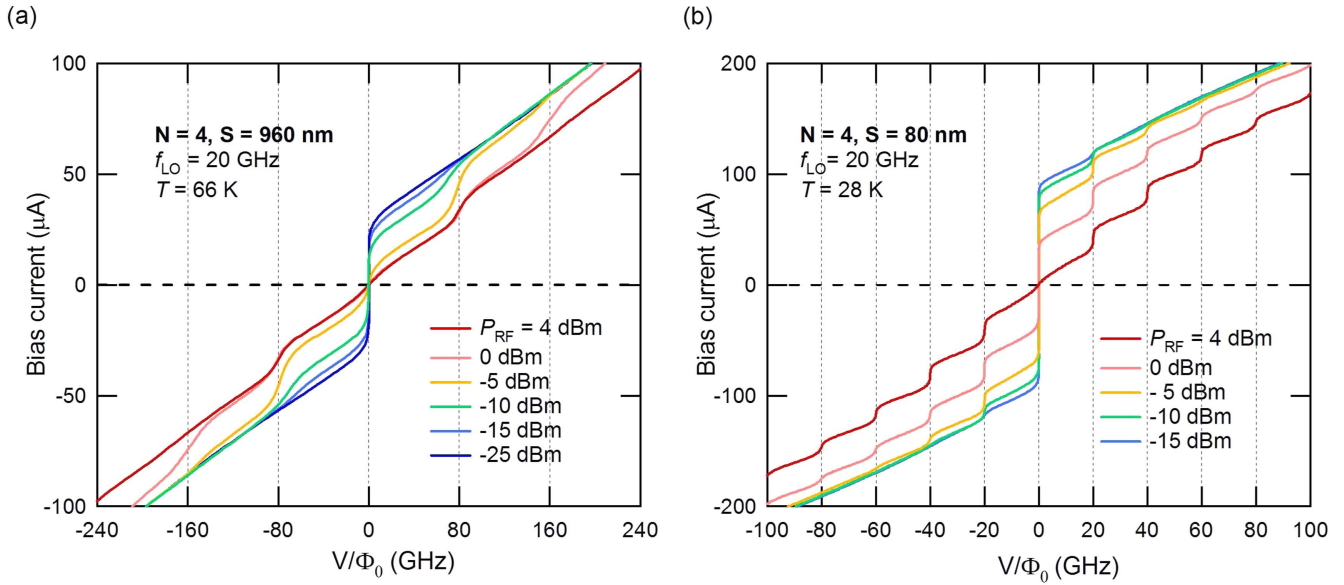
(a)

(b)

Figure 3. DC current versus voltage converted into Josephson frequency—expressed in V/Φ_0 (Φ_0 is the flux quantum)—of 4 JJ arrays with S = 960 nm ((a), *left panel*) and S = 80 nm ((b), right panel) under microwave irradiation at f_{LO} = 20 GHz, for different power P_{RF}. 'Giant Shapiro steps' appear for S = 960 nm. In both cases, I-V characteristics are like.

($4 \times f = 80$ GHz). If the spread in JJ characteristics was too high, we would observed steps at different voltages corresponding to individual junctions. Such giant Shapiro steps have been already observed in other HTSc JJs [18, 25]. Extension to arrays with more JJs, up to a thousand, is currently under investigation.

We performed Josephson mixing experiments with these devices. A weak signal at frequency f_s was applied to a 4 JJ array (S = 960 nm) along with a local oscillator signal at f_{LO}, and the available power at intermediate frequency P_{IF} was measured with a spectrum analyser as a function of an applied DC bias. The result is shown in figure 4(a) for f_{LO} = 20 GHz and f_{LO} = 150 GHz. In both cases $f_s = f_{LO}$-6 GHz. The DC bias V has been converted into a frequency through the Josephson equation ($f = V/\phi_0$, where $\phi_0 = h/2e$ is the flux quantum), and normalised by f_{LO} and the number N of JJs in the array. We observed that P_{IF} is the maximum in the centre of the Shapiro step (only the first one is presented here) for f_{LO} = 20 GHz (black curve), and maximum at the edges of the Shapiro steps for f_{LO} = 150 GHz (orange curve). Such behaviour has already been reported and analysed for single JJ in previous publications [10, 11], and depends on the characteristic frequency $f_c = I_c \cdot R_n/\phi_0$ which rules the dynamics of a JJ, where R_n is the normal state resistance. Since R_n varies with temperature (*cf* figure 2), we used a special procedure to measure it in the Josephson regime below T_J, detailed and justified by Malnou *et al* [10, 11]. $R_n(T)$ is the normal state resistance measured under RF power strong enough to fully suppress the critical current I_c at temperature T. This value coincides with the extrapolation to $T < T_J$ of the resistance curve measured above T_J. For the sample reported in figure 4, $f_c \sim 100$ GHz which is between 20 GHz (black curve) and 150 GHz (orange curve). This shows that JJA mixers with spaced JJ behave like single JJ ones.

This is true for a temperature just below T_J (T = 66 K for the data in figures 3(a) and 4(a)), but more chaotic behaviour is observed when the temperature is lowered. This is shown by observing the mixing patterns at 'high' 66 K and 'low' 60 K temperatures displayed in figures 4(b) and (c) respectively. The 960 nm JJA with 4 JJ has been irradiated with f_s = 14 GHz and f_{LO} = 20 GHz microwaves. The output power at the intermediate frequency P_{IF} is represented in colour scale as a function of both the DC bias voltage (converted into frequency f as before) and the local oscillator power P_{LO}. At high temperature (figure 4(c)), we observe a regular pattern with oscillations separated by 80 GHz (=4 × 20 GHz), as well as a non-monotonic modulation with P_{LO}, as expected. At lower temperature (figure 4(b)), the pattern becomes more fuzzy, with oscillations corresponding to individual JJs or group of JJs. This is because the scattering of JJ parameters is too high. Indeed, sufficient uniformity between junctions is necessary to provide equal optimal biasing for all junctions in the array, and to obtain giant Shapiro steps. Scattering is higher at low temperature because of the rather steep dependence of the critical current I_c with temperature (figure 2). A tiny difference between the critical currents close to T_J translates into an increasing difference as the temperature is lowered.

The first result of this study is that, in a certain range of temperatures, one can benefit from the larger impedance of series-JJA to better match the impedance of the circuits, while preserving good mixing properties in these devices. This does not require phase locking between the JJs [33]. However, mutual phase locking would allow a decrease in the linewidth of the junctions self-oscillation [16], and therefore decrease the noise temperature of the Josephson mixer.
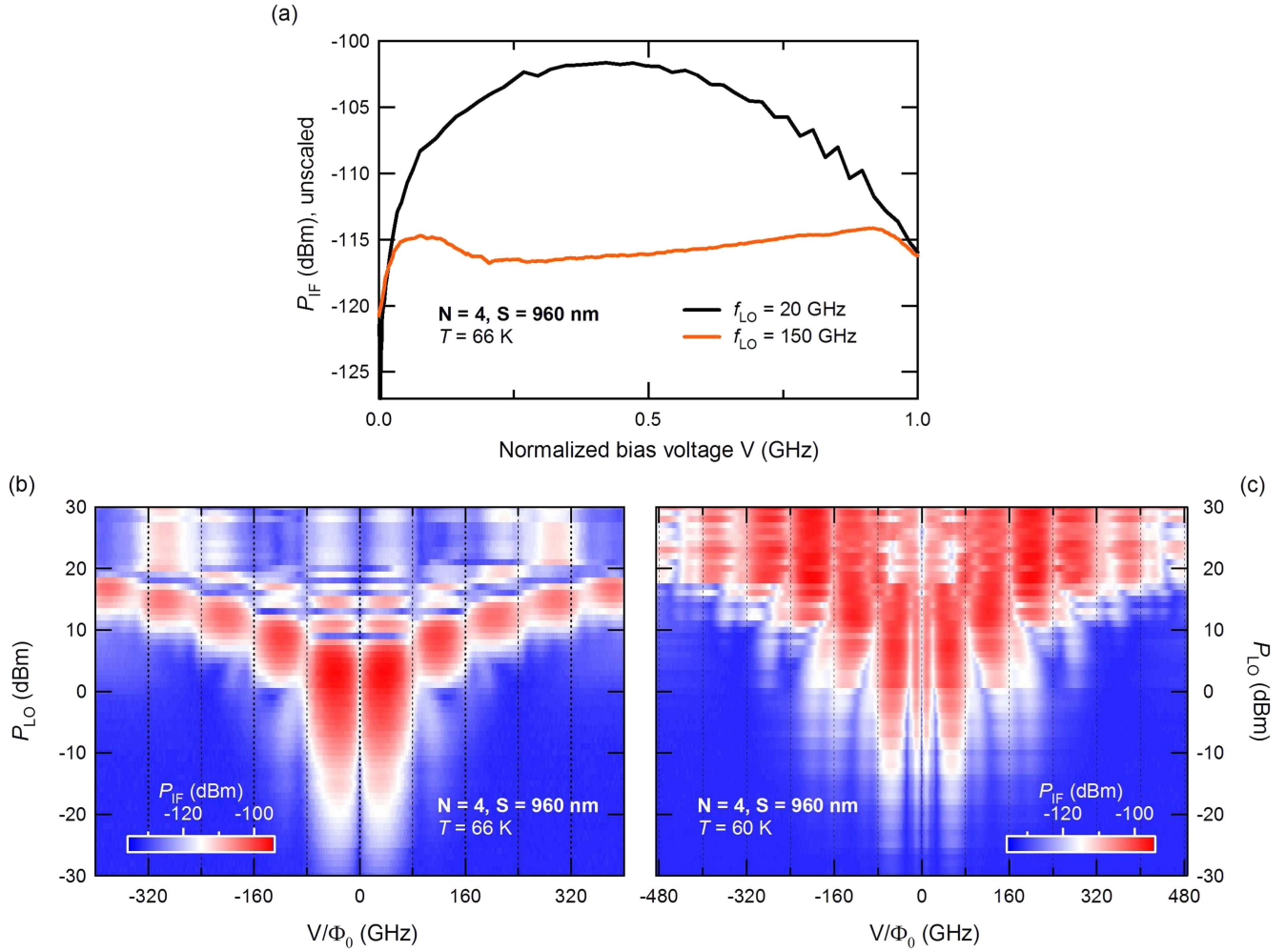
Figure 4. (a) Power at the intermediate frequency $P_{IF} = 6$ GHz as a function of the bias voltage converted into frequency and normalised by the local oscillator frequency f_{LO} and the number of JJs (see text), for a 960 nm spaced 4 JJ array, measured at T = 66 K. In black, f_{LO} = 20 GHz and signal frequency f_s = 14 GHz. In orange, f_{LO} = 150 GHz and f_s = 144 GHz. (b) P_{IF} = 6 GHz on a colour scale as a function of both the bias voltage converted into frequency (see text) and the local oscillator power P_{LO} for the same JJA at T = 66K. Periodicity in frequency is 80 GHz, that is $4 \times 20GHz$: these are 'giant Shapiro steps'. (c) Same data measured at T = 60 K. The pattern is more fuzzy.

Indeed, the local oscillator generates additional noise in the output IF band by down conversion of wide Josephson self-oscillations (see e.g. [15]). The fact that short-range interaction can lead in some cases to mutual phase locking [34–37], and that parameter scattering in our arrays allows us to obtain giant Shapiro steps, encouraged us to put slits as close as possible to keep damaged areas still separated but with shorter virgin areas.

4. Arrays with Josephson junctions 80 nm apart

Samples with 4 and 8 JJ in series—spaced by 80 nm—have been also made and studied. The resistance and the critical current of a typical 4 JJ device are plotted as a function of temperature in figure 2. Surprisingly, the Josephson coupling temperature is significantly lower ($T_J \sim 50$ K) than for 960 nm spaced JJA. The resistance drops to zero in a single step as for 960 nm spaced array. That means that all the JJs have the same T_J, and that the behaviour of the array is not

dominated by a single peculiar JJ. In the opposite case, we should see multiple steps in the R(T) curves since it is a series array. The resistance above T_J is comparable in both types of samples, while I_c(T) shows a less steep increase when the temperature is lowered. When irradiated with $f = 20$ GHz microwaves, regular Shapiro steps displaying a modulation with RF power as expected, develop in the I-V characteristics, whose length correspond to f, and not $4 \times f$ as previously observed in the 960 nm JJA (figure 3(b)). The same behaviour is observed for N = 8 JJA (not shown). This takes place in the whole Josephson temperature range (from 28 K to 50 K). Therefore, JJAs behave as a single JJ with a lower T_J, and a resistance given by the sum of the 4 or 8 JJ in series. This indicates that Josephson coupling is established across the whole array, that is over a very large distance: 400 nm in the 4 JJ case, and 880 nm in the 8 JJ one. While such a long distance Josephson coupling is by itself an interesting experimental fact that deserves a special discussion (see below), let us emphasize another important outcome of this result for high-frequency mixing.

In a mixer, one defines the conversion efficiency η as the ratio between the power at the intermediate frequency P_{IF} and the incident signal power P_s ($\eta = P_{IF}/P_s$). It gives the mixer the ability to efficiently down-convert high-frequency signals into low frequency ones. For standard Josephson mixers [38], η is proportional to $(f_c/f_{LO})^2$, where $f_c = I_c \cdot R_n/\Phi_0$ is the characteristic frequency of the JJ as already defined. Malnou et al recently showed that this applies to YBa$_2$Cu$_3$O$_7$ ion-irradiated JJ [10, 11]. Since η increases quadratically with R_n, the discovery of series JJAs with up to 8 JJ behaving as a single one opens new perspectives to make high efficiency Josephson mixers with HTSc, even if the critical current is lowered.

5. Discussion

As reported above, closely spaced (80 nm) JJA behave as a single JJ where the coupling between superconducting reservoirs takes place over very long distances, up to 880 nm. This behaviour has been observed on the different samples that we measured. We carefully checked that no short-cut could explain such behavior by direct observation of optical pictures. DC and RF measurements, including mixing, show that the whole array behaves as a giant JJ. Indeed, the observed Shapiro steps and the high-frequency mixing can only occur if a phase coherent behavior takes place across the array. That means that some kind of long range proximity effect occurs in HTSc, which is quite surprising in these materials. The proximity effect, firstly introduced by de Gennes [39], describes the coherent propagation of Cooper pairs within non-superconducting regions called 'normal' over a distance ξ_N, which eventually ensures Josephson coupling through this barrier (SNS junctions) at a temperature T_J. The latter decreases as a function of the ratio l/ξ_N, where l is the length of the normal region. Ion-irradiated JJs have been shown to belong to this category [4, 5, 40, 41]. Although this theory was not originally developed for d-wave high-T_c superconductors, it has been successfully used to describe different properties of irradiated YBa$_2$Cu$_3$O$_7$ JJs [5, 16, 41–43]. In case the 'normal' part is a superconductor with a lower critical temperature T_c', as for the damaged region in ion-irradiated JJ, ξ_N goes as $\sqrt{1 + \frac{2}{\ln \frac{T}{T_c'}}}$, and therefore diverges at T_c' [39].

Previous experiments on 5 μm wide bridges irradiated with the same dose ($3 \cdot 10^{13}$ at./cm^2) through slits of different width w showed that the Josephson temperature T_J strongly depends on the width of the slit until it reaches a saturation value [44]. This can be seen in figure 5 where both the resistance R and the critical current I_c have been plotted as a function of temperature for increasing w from 20 to 1000 nm. For $w < 200$ nm, they change significantly while they saturate for $w > 500$ nm. That means that for a critical value w_c, which is between 200 and 500 nm, T_J reaches T_c'. This sets an upper bound for ξ_N under these conditions, which should be around 100-200 nm.

We can thus understand the different features of our present data. Clearly, 960 nm is much larger than ξ_N, and 960 nm spaced JJ are completely independent, while 80 nm ones can have some interaction. In fact, as the proximity effect relates to the propagation of superconducting correlations over ξ_N, the inverse proximity effect relates to normal quasiparticles diffusing in the superconducting part, on the same extension, lowering superconductivity in this region. Therefore, when the distance between two diffusive SNS JJs is smaller than ξ_N, they appear as a single JJ with an apparent increased length. This can be seen in figure 5 where I_c(T) and R(T) for the 80 nm spaced JJA (total length 400 nm for 4 JJ in that case) are close to that of the 500 nm wide JJ of the previous experiment, with almost the same T_J. Note that T_J for the 8 JJA of total length 880 nm is the same because of the saturation effect mentioned above, and that T_J for the 960 nm spaced JJA is close to that of the single 20 nm wide one.

In the literature, only two series of experiments have been reported with closely spaced YBa$_2$Cu$_3$O$_7$ planar JJs. Using direct e-beam irradiation to fabricate JJs, Booij et al [30] studied the electro-dynamics of two JJs separated by 75 nm when an external magnetic field is applied. They essentially discuss the current redistribution within the electrodes that form the JJ, and its consequences on the Fraunhofer pattern. However, there are no measurements at finite frequency that we can compare with. Chen et al used an ion-irradiation technique very close to ours, to make pairs and arrays of JJ with spacing ranging from 125 nm to 800 nm [26, 45], and studied their AC response. They observed giant Shapiro steps in structures with inter-JJ distances larger than 150 nm. Our results on 960 nm spaced JJs are fully compatible with theirs. When the distance between JJs is smaller than 150 nm, Chen et al report on a different and very interesting behaviour [45]. At low RF power, samples display giant Shapiro steps corresponding to independent JJs. However, at high RF power, it behaves like a single JJ, exactly as our 80 nm spaced JJA. This behaviour can be understood in the frame that we proposed above. The distance between JJs in the array of Chen et al is 150 nm, that is on the order of ξ_N, may be a little bit larger: the JJ are thus decoupled. But at the same time, the inverse proximity effect decreases the strength of superconductivity in the region between the JJs. Increasing RF power introduces incoherent processes (analogous to temperature), and this region becomes a weak link as well. The whole structure behaves as a single JJ.

Indeed, these are qualitative arguments only, and one needs to understand in more detail the mechanism underlying this surprising result. A microscopic theory based on semi-classical Usadel equations can be developed [44]. Recently a model has been proposed by Kresin et al [46, 47], to explain a giant proximity effect reported in c-axis transport measurement in cuprates [48]. The main idea is that two distanced superconductors separated by a chain of superconducting islands with their own pairing functions might form a single Josephson junction if their pairing amplitudes overlap. Application of this theory to the present data needs to be done.
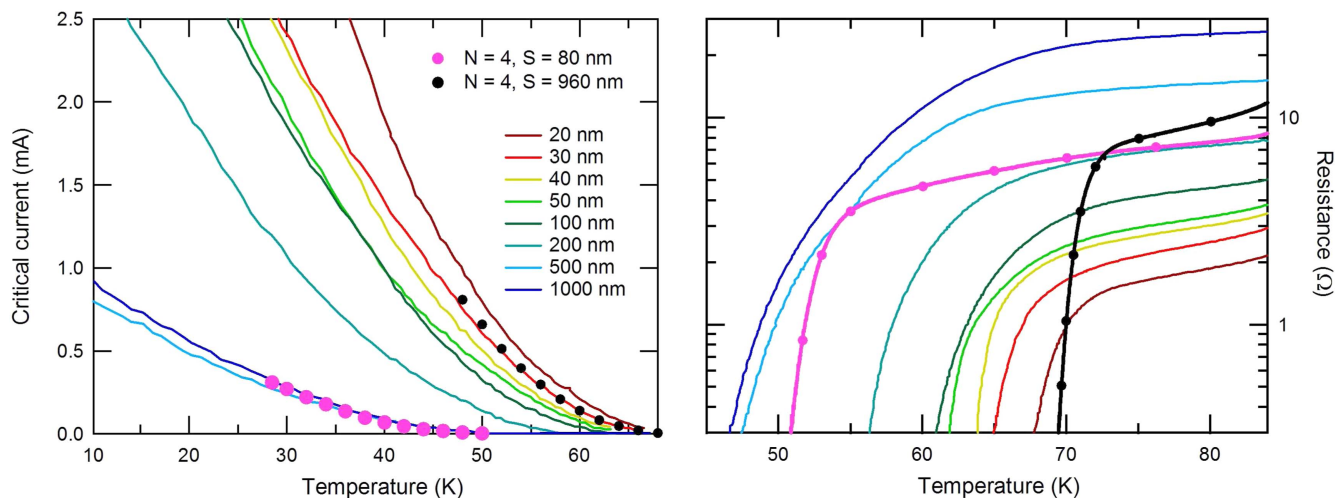
Figure 5. Temperature dependence of the critical current I_c (left panel) and the resistance R (right panel) of $YBa_2Cu_3O_7$ 5 μm wide bridges irradiated through slits of different width w with the same dose ($3 \cdot 10^{13}$ at./cm^2). w ranges from 20 to 1000 nm (see colour code in the panel). For comparison, I_c(T) and R(T) for the 4 JJ arrays are also shown, for S = 80 nm (pink solid circle and line) and 960 nm (black solid circle and line).

6. Conclusion

Josephson mixing on giant Shapiro steps of ion-irradiated Josephson junction arrays has been demonstrated. Replacing a single junction by an array will allow us to improve the impedance mismatch of previously reported Josephson mixers [10, 11]. To improve the noise temperature of the mixer as well as for many other possible applications, phase locking between junctions in an array is necessary. We believe that for this particular type of junction, short-range interaction may be a promising approach to achieve phase synchronisation.

The reported experiments showed that 80 nm spaced JJAs behave as single junction. From an application point of view, this offers an interesting possibility to increase the I_cR_N product of ion-irradiated JJs, and correlatively the conversion efficiency of the Josephson mixers. On the basic science side, the long range proximity effect over distances up to 880 nm observed here can be explained by general arguments taking into account the inverse proximity effect and the estimated value of the normal coherence length.

Acknowledgments

ORCID iDs

A Sharafiev ⬤ https://orcid.org/0000-0002-8780-9261
C Feuillet-Palma ⬤ https://orcid.org/0000-0002-8389-5756

References

[1] Du J, Weily A R, Gao X, Zhang T, Foley C P and Guo Y J 2016 HTS step-edge Josephson junction terahertz harmonic mixer *Supercond. Sci. Technol.* **30** 024002

[2] Snezhko A V, Gundareva I I, Lyatti M V, Volkov O Y, Pavlovskiy V V, Poppe U and Divin Y Y 2017 Terahertz Josephson spectral analysis and its applications *Supercond. Sci. Technol.* **30** 044001

[3] Du J, Pegrum C M, Gao X, Weily A R, Zhang T, Guo Y J and Foley C P 2017 Harmonic mixing using a HTS Step-edge Josephson junction at 0.6 THz frequency *IEEE Trans. Appl. Supercond.* **27** 1500905

[4] Katz A S, Sun A, Woods S I and Dynes R C 1998 Planar thin film $YBa_2Cu_3O_{7-\delta}$ Josephson junctions via nanolithography and ion damage *Appl. Phys. Lett.* **72** 2032

[5] Bergeal N, Grison X, Lesueur J, Faini G, Aprili M and Contour J 2005 High-quality planar high-T_c Josephson junctions *Appl. Phys. Lett.* **87** 102502

[6] Tinchev S 1990 Investigation of RF SQUIDs made from epitaxial YBCO films *Supercond. Sci. Technol.* **3** 500

[7] Bergeal N, Lesueur J, Faini G, Aprili M and Contour J 2006 High T_c superconducting quantum interference devices made by ion irradiation *Appl. Phys. Lett.* **89** 112515

[8] Cybart S, Anton S, Wu S, Clarke J and Dynes R 2009 Very large scale integration of nanopatterned $YBa_2Cu_3O_{7-\delta}$ Josephson junctions in two-dimensional array *Nano Letters* **9** 3581

[9] Ouanani S, Kermorvant J, Ulysse C, Malnou M, Lemaître Y, Marcilhac B, Feuillet-Palma C, Bergeal D, Crété N and Lesueur J 2016 High T_c superconducting quantum interference filters (SQIFs) made by ion irradiation *Supercond. Sci. Technol.* **29** 094002

[10] Malnou M *et al* 2012 Toward terahertz heterodyne detection with superconducting Josephson junctions *Appl. Phys. Lett.* **101** 233505

[11] Malnou M, Feuillet-Palma C, Ulysse C, Faini G, Febvre P, Sirena M, Olanier L, Lesueur J and Bergeal N 2014 High-T_c superconducting Josephson mixers for terahertz heterodyne detection *J. Appl. Phys.* **116** 074505

[12] Cybart S, Chen K, Cui Y, Li Q, Xi X and Dynes R 2006 Planar MgB_2 Josephson junctions and series arrays via nanolithography and ion damage *Appl. Phys. Lett.* **88** 012509

[13] Cybart S, Cho E, Wong T, Björn H, Ma M, Huynh C and Dynes R 2015 Nano Josephson superconducting tunnel junctions in YBa$_2$Cu$_3$O$_{7-\delta}$ directly patterned with a focused helium ion beam *Nat. Nanotechnol.* **10** 598

[14] Cho E, Ma M, Huynh C, Pratt K, Paulson D, Glyantsev V, Dynes R and Cybart S 2015 YBa$_2$Cu$_3$O$_{7-\delta}$ superconducting quantum interference devices with metallic to insulating barriers written with a focused helium ion beam *Appl. Phys. Lett.* **106** 252601

[15] Jain A, Likharev K, Lukens J and Sauvageau J 1984 Mutual phase-locking in Josephson junction arrays *Phys. Rep.* **109** 309

[16] Sharafiev A, Malnou M, Feuillet-Palma C, Ulysse C, Febvre P, Lesueur J and Bergeal N 2016 Josephson oscillation linewidth of ion-irradiated YBa$_2$Cu$_3$O$_7$ junctions, *Supercond. Sci. Technol.* **29** 074001

[17] Benz S and Hamilton C 1996 A pulse-driven programmable Josephson voltage standard *Appl. Phys. Lett.* **68** 3171

[18] Klushin A, Prusseit W, Sodtke E, Borovitskii S I, Amatuni L E and Kohlstedt H 1996 Shunted bicrystal Josephson junctions arrays for voltage standards *Appl. Phys. Lett.* **69** 1634

[19] Benz S, Hamilton C, Burroughs C, Harvey T, Lawrence A and Przybysz J 1998 Pulse-driven Josephson digital/analog converter *IEEE Trans. Appl. Supercond.* **8** 42

[20] Konopka J, Wolff I, Beuven S and Siege M 1995 Mixing and detection in YBaCuO step-edge Josephson junction arrays up to 670 GHz *IEEE Trans. Appl. Supercond.* **5** 2443

[21] Tsuru K, Miyahara K and Suzuki M 1995 Millimeter wave response of Josephson junction arrays using a waveguide to microstrip line converter *Advances in Superconductivity-VIII* ed H Hayakawa and Y Enomoto (Berlin: Springer) p 1171

[22] Barbara P, Cawthorne A, Shitov S and Lobb C 1999 Stimulated emission and amplification in Josephson junctions arrays *Phys. Rev. Lett.* **82** 1963

[23] Han S, Bi B, Zhang W and Lukens J 1994 Demonstration of josephson effect submillimeter wave sources with increased power *Appl. Phys. Lett.* **64** 1424

[24] Kunkel G *et al* 1997 Millimeter-wave radiation in High-T_c Josephson junctions *IEEE Trans. Appl. Supercond.* **7** 3339

[25] Klushin A, He M, Levitchev M, Kurin N and Klein V V 2008 Optimization of the coupling of mm wave power to arrays of high-T_c Josephson junctions *J. Phys.: Conf. Ser.* **97** 012268

[26] Chen K, Cybart S and Dynes R 2004 Planar thin film YBa$_2$Cu$_3$O$_7$ Josephson junction pairs and arrays via nanolithography and ion damage *Appl. Phys. Lett.* **85** 2863

[27] Cybart S, Wu S, Anton S, Siddiqi I, Clarke J and Dynes R 2008 Series array of incommensurate superconducting quantum interference devices from YBa$_2$Cu$_3$O$_7$ ion damage Josephson junctions *Appl. Phys. Lett.* **93** 182502

[28] Cybart S A *et al* 2014 Large voltage modulation in magnetic field sensors from two-dimensional arrays of Y-Ba-Cu-O nano Josephson junctions *Appl. Phys. Lett.* **104** 062601

[29] Cybart S, Chen K and Dynes R 2005 Planar MgB$_2$ Josephson junctions and series arrays via nanolithography and ion damage *IEEE Trans. Appl. Supercond.* **15** 241

[30] Booij W E, Pauza A J, Moore D F, Tarte E J and Blamire M G 1997 Electrodynamics of closely coupled YBa$_2$Cu$_3$O$_{7-\delta}$ junctions *IEEE Trans. Appl. Supercond.* **7** 3025

[31] Bindslev Hansen J and Lindelof P 1984 Static and dynamic interactions beween Josephson junctions *Rev. Mod. Phys.* **56** 431

[32] Bergeal N, Lesueur J, Sirena M, Faini G, Aprili M, Contour J P and Leridon B 2007 Using ion irradiation to make high-T_c Josephson junctions *J. Appl. Phys.* **102** 083903

[33] Kuzmin L, Likharev K and Migulin V 1981 Microwave receivers using SQUIDs and Josephson junction arrays *IEEE Trans. Magn.* **17** 822

[34] Lindelof P, Hansen B, Mygind J, Pedersen N and Sørensen O 1977 Coherent Josephson radiation from an array of two Dayem briges *Phys. Lett.* A **60** 451

[35] Li H, Ono R, Vale L, Rudman D and Liou S 1999 Interactions between bicrystal Josephson junctions in a multilayer structure *IEEE Trans. Appl. Supercond.* **9** 3417

[36] Kleiner R, Steinmeyer F, Kunkel G and Müller P 1992 Intrinsic Josephson effects in Bi$_2$Sr$_2$CaCu$_2$O$_8$ single crystals *Phys. Rev. Lett.* **68** 2394

[37] Carapella G, Costabile G, Petraglia A, Pedersen N and Mygind J 1996 Phase locked fluxon-antifluxon states in stacked Josephson junctions *Appl. Phys. Lett.* **69** 1300

[38] Barone A and Paterno G 1982 *Physics and Applications of the Josephson Effect* (New York: Wiley-Interscience)

[39] de Gennes P 1964 Boundary effects in superconductors *Rev. Mod. Phys.* **36** 225

[40] Tinchev S 1994 Current-phase relation in high-T_c weak links made by oxygen-ion irradiation *Physica* C **222** 173

[41] Katz A S, Woods S I and Dynes R C 2000 Transport properties of high-T_c planar Josephson junctions fabricated by nanolithography and ion implantation *J. Appl. Phys.* **87** 2978

[42] Pauza A, Booij W, H K, Moore D, Blamire M, Rudman D A and Vale L R 1997 Electron-beam damaged high-temperature superconductor Josephson junctions *J. Appl. Phys.* **5612**

[43] Booij W, Pauza A, Tarte E, Moore D and Blamire M 1997 Proximity coupling in high-T_c Josephson junctions produced by focused electron beam irradiation *Phys. Rev.* B **55** 1634

[44] Wolf T 2010 Étude de nanojunctions Josephson à haute température critique en vue d'applications térahertz *PhD Thesis* University Pierre and Marie Curie (in French)

[45] Chen K, Cybart S and Dynes R 2005 Study of closely spaced YBa$_2$Cu$_3$O$_{7-\delta}$ Josephson junction pairs *IEEE Trans. Appl. Supercond.* **15** 149

[46] Kresin V, Ovchinnikov Y and Wolf S 2003 Giant Josephson proximity effect *Appl. Phys. Lett.* **83** 722

[47] Kresin V, Ovchinnikov Y and Wolf S 2006 Inhomogeneous superconductivity and the pseudogap state of novel superconductors *Phys. Rep.* **431** 231

[48] Bozovic I, Logvenov G, Verhoeven M, Caputo P, Goldobin E and Beasley M 2004 Giant proximity effect in cuprate superconductors *Phys. Rev. Lett.* **93** 157002